16ème Congrès Français d'Acoustique
11-15 Avril 2022, Marseille

Estimating the depth of a buried polyethylene pipe by comparing propagation models

W. Xerri [a,c], G. Saracco [a], A. Ribodetti [b], L. Zomero[c] et P. Picon[c]

[a] CNRS-UMR7330 CEREGE, AMU, CdF, Europole de l'Arbois, BP 80, 13545 Aix-En-Provence Cedex 4, France
[b] IRD-UR082 CNRS-UMR7329 Geoazur, Campus Azur Université et observatoire de la côte d'azur, 250 rue Albert Einstein CS 10269, 06905 Sophia Antipolis, France
[c] MADE-SA, 167 Impasse de la Garrigue, 83210 La Farlède, France

xerri@cerege.fr, saracco@cerege.fr, Alessandra.ribodetti@geoazur.unice.fr, l.zomero@made-sa.com, p.picon@made-sa.com

In civil engineering, one of the crucial problems is the location of buried polyethylene pipes. For this type of material, electromagnetic waves are less suitable than acoustic waves (e.g. the necessity to introduce a metal cable into the pipeline making the method invasive, difficulty in differentiating between a gas pipe and a water pipe). By injecting an acoustic signature into the pipe it possible to estimate the passage of the plumb of the pipe, by considering the pipe as a secondary vibrating source. Our work aims to estimate the depth of these pipes by acoustic method and in a non-destructive way. For this we have developed a system to take real data measurements. From antenna processing methods (MUSIC algorithm called "high resolution") that we have adapted to our problematic, we obtain an estimate of the parameters of interest. Promising results have been obtained on real data from a semi-controlled test area by considering a weakly heterogeneous semi-infinite medium with an average velocity. One of the main problems is that we have, a priori, no knowledge of the propagation medium. It can change drastically from one place of application to another. The challenge is the modeling of acoustic propagation, on a meter scale, in heterogeneous soil with vertical (trench). We present here different propagation simulations applied to our problem. A first modeling is to consider two slightly heterogeneous media, vertically stratified, each with an average speed of propagation, considering the ray theory (time modeling). The second will be based on finite difference propagation of the complete waves field (Operto et al., Geophysics, 2009) including the trench. The goal is to compare the two models on the scale of our problem and to study the accuracy of the depth estimate that we can reach (Cramer Rao bound).

1 Introduction

The detection and location of buried pipes is an important issue, especially to update the mapping of networks in accordance with new standards. Our study is restricted to polyethylene pipes which is a non-conductive material. Different methods exist to trace and locate pipes [1,2]. Our study focuses on an acoustic method. The principle is to inject an acoustic source signal into the pipe and to observe the signals received by receivers placed on the ground surface. The advantage of these methods based on the acoustic excitation of the pipe is to be able to discern the pipe of interest in a dense network. Tools based on this method allow to estimate the passage of the pipe plumb but do not provide any information on the depth. The objective of this work is to develop a method to estimate the depth of pipes in a non-destructive and non-invasive way and with an accuracy of 10 cm. It should be noted that in this problem we have different unknown parameters that must be taken into account to estimate the depth. We have no information on the propagation medium. This means that the propagation speeds in the medium are unknown. It is interesting to note also the scale at which we work. The distances between the pipe and the receivers are in the order of meter.

This article follows on from work already presented in which the modeling of the acoustic wave propagation medium is considered as a homogeneous medium [3]. From the delay times between the sensors we want to estimate the depth. We had tested the depth estimation with the homogeneous medium modeling on real data. For a majority of the measurements performed on the test area we had, the results were of the desired accuracy (10 cm). These results were obtained by adapting the MUSIC algorithm to our problem. However, we are aware that the pipe buried in this test area is in a trench. There is therefore a change of medium. In the context of these tests we can imagine that the two media were close.

Now we want to make the model evolve so that it takes into account two propagation media, and we will consider two strongly different media. We consider here a model covering a larger number of situations, by integrating a vertical variation of the medium between the inside of the trench where the pipe is buried, and the outside of the trench, for two propagation models, one based on a ray tracing code (time modeling) according to the Snell-Descartes laws, the other taking into account a finite difference model of the complete wave field [4].

2 Geometric configuration of the problem

In agreement with studies on vibro-acoustic propagation in pipes [5] we consider the pipe as a cylindrical line source. From this consideration and the resulting symmetries, we model the problem in a plane radial to the pipe. The sensors are distributed perpendicular to the pipe (Figure 1) and the pipe section is considered as a point source.

In this paper, we propose to focus on a model with two propagation media. The idea is to take into account the change of medium between inside and outside the trench. We therefore consider a vertically stratified medium, with an average propagation velocity V_1 inside the trench and an average velocity V_2 outside.

We assume weakly heterogeneous environments, but it is obvious that the propagation environment is more complex in an urban context, particularly due to the presence of a layer of bitumen covering the ground or the protective layer of sand (granular environment) surrounding the pipe. The objective is to obtain a parametric model allowing, from travel time estimate, to estimate the depth.

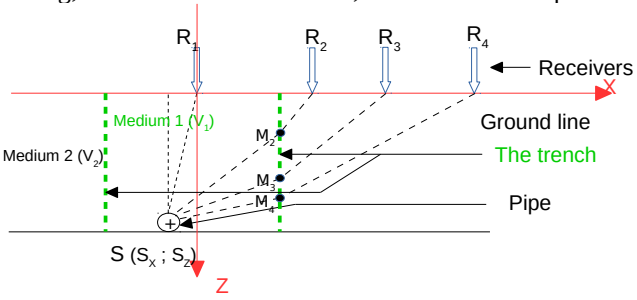

Figure 1 : Scheme of model

3 Reasoning on signal traveling times from ray theory

In this part we reason in travel time between the source and the receivers by considering the Snell-Descartes law at the interface between the two media.

3.1 Description of the model

The principle is to determine the travel time of the signal between the source S and the receiver R_i. To do this it is necessary to calculate the point of interface between the two media M_i which respects the law of Snell-Descartes.

$$\sin(\phi_1)=\frac{V_1}{V_2}\ \sin(\phi_2) \quad (1)$$

With ϕ_1 the angle of incidence, ϕ_2 the angle of refraction, V_1 the velocity in medium 1 (inside the trench) and V_2 the velocity in medium 2 (outside the trench).

For each receiver R_i corresponds an interface point M_i.

3.2 Cramer-Rao bound

The Cramer-Rao bound gives an idea of the accuracy of depth estimation in relation to our time modeling [6].

In order to calculate this bound we need to express the coordinates of the interface point M_i in terms of our parameters of interest : S_X the X coordinate of the source, S_Z the Z coordinate of the source, V_1 the velocity inside the trench and V_2 the velocity outside the trench. We note θ the vector of these parameters of interest.

$$\theta = [S_X\ S_Z\ V_1\ V_2]^T \quad (2)$$

We consider that the position of the interface between the two media along the X axis, M_X is known. We therefore have to express M_{iZ} the Z coordinate of M_i.

Taking equation (1) again, we have as a starting equation

$$\frac{S_Z - M_{iZ}}{|SM_i|} = \frac{M_{iZ}}{|M_iR_i|}\ \frac{V_1}{V_2} \quad (3)$$

This is equivalent to solving the following 4th order equation :

$$\begin{aligned} &M_Z^4\left[V_2^2-V_1^2\right]\\ &+M_Z^3\left[-2R_ZV_2^2-2S_ZV_2^2+2S_ZV_1^2\right]\\ &+M_Z^2\left[S_Z^2V_2^2+R_Z^2V_2^2+V_2^2(R_X-M_X)^2+4R_ZS_ZV_2^2-S_Z^2V_1^2-V_1^2(M_X-S_X)^2\right]\\ &+M_Z\left[-2R_ZS_Z^2V_2^2-2S_ZR_Z^2V_2^2-2S_ZV_2^2(R_X-M_X)^2\right]\\ &+\left[R_Z^2S_Z^2V_2^2+S_Z^2V_2^2(R_X-M_X)^2\right] = 0 \end{aligned} \quad (4)$$

By identification, we can write

$$M_{iZ}^4\ m_1 + M_{iZ}^3\ m_2 + M_{iZ}^2\ m_3 + M_{iZ}\ m_4 + m_5 = 0 \quad (5)$$

Solving the equation, we obtain

$$M_{iZ} = \frac{\sqrt{A} - \sqrt{A - 2\left(p + A + \frac{q}{\sqrt{A}}\right)}}{2} - \frac{m_2}{4m_1} \quad (6)$$

with

$$A = \left(\frac{-R + \sqrt{R^2 + \frac{4Q^3}{27}}}{2}\right)^{1/3} - \frac{Q}{3\left(\frac{-R + \sqrt{R^2 + \frac{4Q^3}{27}}}{2}\right)^{1/3}} - \frac{2p}{3} \quad (7)$$

$$Q = -\frac{p^2}{3} - 4r \quad (8) \qquad R = \frac{8rp}{3} - \frac{2p^3}{27} - q^2 \quad (9)$$

$$p = \frac{m_3}{m_1} - \frac{3m_2^2}{8m_1^2} \quad (10) \qquad q = \frac{m_4}{m_1} - \frac{m_2m_3}{2m_1^2} + \frac{m_2^3}{8m_1^3} \quad (11)$$

$$r = \frac{m_5}{m_1} - \frac{m_2m_4}{4m_1^2} + \frac{m_2^2m_3}{16m_1^3} - \frac{3m_2^4}{256m_1^4} \quad (12)$$

We also need to calculate the gradient of M_{iZ} as a function of our parameters of interest which we will note $\nabla_\theta(M_{iZ})$. We will express the Cramer-Rao bound in terms of $\nabla_\theta(M_{iZ})$.

The Cramer-Rao bound, noted here CRB, is calculated according to the Fisher information matrix, noted F.

$$CRB(\theta) = F^{-1}(\theta/\tau_{1i}) \quad (13)$$

with τ_{1i} the relative delay time between the sensors 1 and i.

To express the τ_{1i} two cases are possible :

- If R_i is inside the trench this returns us to the case of a homogeneous medium.

$$\tau_{1i} = \frac{|SR_i| - |SR_1|}{V_1} \quad (14)$$

- If R_i is outside the trench

$$\tau_{1i} = \frac{|SM_i| - |SR_1|}{V_1} + \frac{|M_iR_i|}{V_2} \quad (15)$$

Here we are interested in the case of equation (15).

We express the Fisher information matrix

$$F(\theta/\tau_{1i}) = \sum_{i=2}^{N} \frac{1}{Var(\tau_{1i})}\ \nabla_\theta(\tau_{1i})\ \nabla_\theta^T(\tau_{1i}) \quad (16)$$

with N the number of sensors and $Var(\tau_{1i})$ the variance of the relative delay time between sensor 1 and i.

Let's focus on the calculation of the gradient of a relative delay time. From equation (15) we have

$$\nabla_\theta(\tau_{1i}) = \nabla_\theta\left(\frac{|SM_i|}{V_1}\right) - \nabla_\theta\left(\frac{|SR_1|}{V_1}\right) + \nabla_\theta\left(\frac{|M_iR_i|}{V_2}\right) \quad (17)$$

By decomposing the calculation we obtain the following expressions

$$\nabla_\theta\left(\frac{|SR_1|}{V_1}\right) = \left[\frac{S_X - R_{1X}}{V_1|SR_1|}\ \ \frac{S_Z - R_{1Z}}{V_1|SR_1|}\ \ \frac{-|SR_1|}{V_1^2}\ \ 0\right]^T \quad (18)$$

$$\nabla_\theta\left(\frac{|SM_i|}{V_1}\right)=\begin{bmatrix}\dfrac{(S_X-M_{iX})-(S_Z-M_{iZ})\dfrac{\partial}{\partial S_X}M_{iZ}}{V_1\,|SM_i|}\\[2ex]\dfrac{(S_Z-M_{iZ})\left(1-\dfrac{\partial}{\partial S_Z}M_{iZ}\right)}{V_1\,|SM_i|}\\[2ex]\dfrac{-V_1(S_Z-M_{iZ})\dfrac{\partial}{\partial V_1}M_{iZ}-|SM_i|^2}{V_1^2\,|SM_i|}\\[2ex]\dfrac{-(S_Z-M_Z)\dfrac{\partial}{\partial V_2}M_{iZ}}{V_1\,|SM_i|}\end{bmatrix} \quad (19)$$

$$\nabla_\theta\left(\frac{|M_iR_i|}{V_2}\right)=\begin{bmatrix}\dfrac{(M_{iZ}-R_{iZ})\dfrac{\partial}{\partial S_X}M_{iZ}}{V_2\,|M_iR_i|}\\[2ex]\dfrac{(M_{iZ}-R_{iZ})\dfrac{\partial}{\partial S_Z}M_{iZ}}{V_2\,|M_iR_i|}\\[2ex]\dfrac{(M_{iZ}-R_{iZ})\dfrac{\partial}{\partial V_1}M_{iZ}}{V_2\,|M_iR_i|}\\[2ex]\dfrac{V_2(M_{iZ}-R_{iZ})\dfrac{\partial}{\partial V_2}M_{iZ}-|M_iR_i|^2}{V_2^2\,|M_iR_i|}\end{bmatrix} \quad (20)$$

In our case the receivers are all placed on the ground so the $R_{iZ} = 0$.

Now that we have calculated the Cramer-Rao bound we can vary our parameters and observe the impact on the depth estimation accuracy.

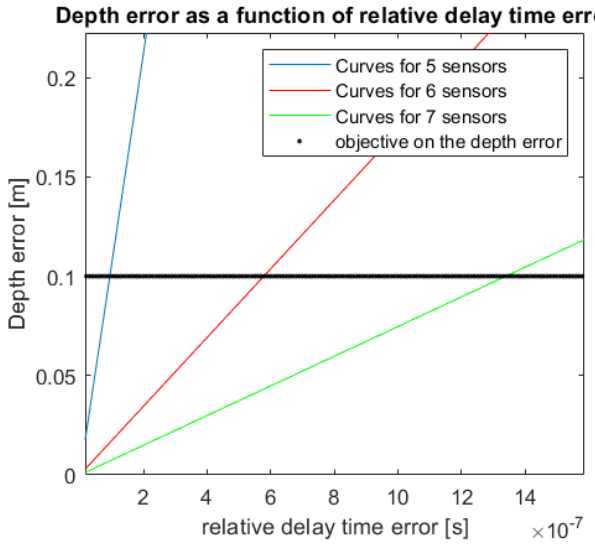

Figure 2 : Depth error as a function of relative delay time error

For example we consider the following case: the sensors are spaced of 0.2 m, the X coordinate of the source S_X =0, the Z coordinate of the source S_Z = 0.8 m, the velocity inside the trench V_1 = 500 m/s, the velocity outside the trench V_2 = 700 m/s, the X coordinate of the interface points between the media M_X = 0.35 m.

We note (Figure 2) that to obtain an accuracy of 10 cm on the depth estimation we must, with 5 sensors, have an accuracy on the relative delay times of the order of 10^{-7} s, with 6 sensors $\frac{1}{2}\ 10^{-6}$ s and with 7 sensors 10^{-6} s. The more sensors we add, the more error we can tolerate on the estimation of relative delay times.

4 Comparisons of arrival times estimate with finite difference modeling of the full wave field

In this section, we compare the time estimates obtained with the method presented in section 3 with a finite difference wave propagation simulation in a simple model. Firstly, we recall the basis of the classic approach of wave propagation based on of the acoustic and isotropic finite difference approach, then we present a test of propagation in simple models to perform comparison of arrival times.

4.1 Finite Difference Modeling of Acoustic Isotropic Wave Propagation

In this study we used the acoustic and isotropic version of the code developed by Operto et al. [4] from the original formulation proposed by Jean Virieux [7].

The 2D velocity-stress (21) is expressed as an equation of order one in the following form

$$\begin{cases}\dfrac{\partial v_x(\mathbf{x},t)}{\partial t} = b(\mathbf{x})\dfrac{\partial p(\mathbf{x},t)}{\partial x} + f_x\\[2ex]\dfrac{\partial v_z(\mathbf{x},t)}{\partial t} = b(\mathbf{x})\dfrac{\partial p(\mathbf{x},t)}{\partial z} + f_z\\[2ex]\dfrac{\partial p(\mathbf{x},t)}{\partial t} = \kappa(\mathbf{x})\left(\dfrac{\partial v_x(\mathbf{x},t)}{\partial x}+\dfrac{\partial v_z(\mathbf{x},t)}{\partial z}\right)\end{cases} \quad (21)$$

In this system v and p are the velocity and the pressure respectively, $b = \frac{1}{\rho}$ is the buoyancy of the medium (with ρ the density) and $\kappa = \rho c^2$ is the compressibility. f_x and f_z are the components of the vertical and horizontal forces and correspond to the source terms. The density ρ is estimated from the velocity model by using the empirical Gardner law [8] which is valid for short offset data [9]. To solve numerically this system of equations the time and space are discretized by using a step Δt , Δx and Δz respectively. The index are *n* for time and *i* and *j* for the directions *x* and *z*. The discretization is performed on a cartesian grid $\Delta x = \Delta z = h$. As usual, to optimize the computational cost the velocity field is discretized over grid shifted in time $\frac{\Delta t}{2}$ and a half step in space along *x* and *z*.

The discretized system of equations is

$$\begin{cases} \dfrac{\upsilon_{x_{i+1/2,j}}^{n+1/2} - \upsilon_{x_{i+1/2,j}}^{n-1/2}}{\Delta t} = \dfrac{b_{i+1/2,j}}{h}\left(p_{i+1,j}^{n} - p_{i,j}^{n} \right) + f_{x\,i+1/2,j}^{n} \\ \dfrac{\upsilon_{z_{i,j+1/2}}^{n+1/2} - \upsilon_{z_{i,j+1/2}}^{n-1/2}}{\Delta t} = \dfrac{b_{i,j+1/2}}{h}\left(p_{i,j+1}^{n} - p_{i,j}^{n} \right) + f_{zi,j+1/2}^{n} \\ \dfrac{p_{i,j}^{n+1} - p_{i,j}^{n}}{\Delta t} = \dfrac{\kappa_{i,j}}{h}\left(\upsilon_{x_{i+1/2,j}}^{n+1/2} - \upsilon_{x_{i-1/2,j}}^{n+1/2} + \upsilon_{z_{i,j+1/2}}^{n+1/2} - \upsilon_{z_{i,j-1/2}}^{n+1/2} \right) \end{cases} \quad (22)$$

From a practical point of view, the spatial discretization is of order 4, which is a good compromise between accuracy and efficiency. Indeed, the sampling step h depends on the wavelength and the order of the discretization. By dispersion analysis, a numerical anisotropy is highlighted [10,11]. In the simulation, the numerical phase velocity depends on the incidence angle ϕ of the plane wave. According to [4,10], the choice of 5 points per wavelength in the order 4 corresponds to the limit for the speed to be independent of the angle ϕ (precision). In addition, this number of points satisfies the Shannon-Nyquist theorem without exceeding too much the required number of points (efficiency) [10] and the grid h of the model satisfies

$$h \leq \frac{c_{min}}{5 f_{max}} \quad (23)$$

where c_{min} is the minimum velocity and f_{max} the maximum frequency of the wave.

The stability analysis gives a criterion on the time sampling step Δt also dependent on the discretization order. In the case of order 4, the time step is conditioned by [10]

$$\Delta t \leq \sqrt{\frac{3}{8}}\,\frac{h}{c_{max}} \quad (24)$$

where c_{max} is the maximum velocity.

In reality, the waves propagate outside the study area. In a numerical model, it is then necessary to define boundary conditions that prevent side effects. The most used method for this is the definition of an absorbing edge around the digital grid. This PML (Perfectly Matched Layer) is defined by two functions γ_x and γ_z which play the role of attenuating factors for propagation in directions x and z [12]. In general, the number of PML points N_{PML} is determined by

$$N_{PML} = \frac{2\lambda_{min}}{h} \quad (25)$$

where λ_{min} is the minimum wavelength.

The boundary conditions at the surface are that of a free surface :

$$\begin{cases} p(x, z=0, t) = 0 \\ \upsilon_x(x, z=0^-, t) = \upsilon_x(x, z=0^+, t) \\ \upsilon_z(x, z=0^-, t) = \upsilon_z(x, z=0^+, t) \end{cases} \quad (26)$$

The symmetry of the velocity around the free surface ensures that the pressure is 0 at any time t and the anti-symmetry of the pressure ensures the symmetry of the velocity.

4.2 Numerical tests

In the first test, we consider a homogeneous medium characterized by constant velocity v = 500 m/s of dimensions x = 0.7 m and z = 1.5 m. We consider the Ricker function (Figure 3.a) with the central frequency of 500 Hz (Figure 3.b). Then we shifted this function in order to obtain the maximum at time t = 0 s. We use this function as a source for our numerical experiment (Figure 3.c). A set of 30 receivers is located at the bottom of the model at z = 1.5 m. The first receiver is located at x = 0.35 m and z = 1.5 m, the distance between receivers is 0.01 m. The vertical velocity wavefield recovered at the receivers is presented in Figure 3.d. The estimated arrival times computed by using the method presented in section 3 are plotted on Figure 3.d (blue dashed curve). We can observe a very good fit for short offsets and acceptable fit for long offsets because of the broadening of the signal associated with the propagation.

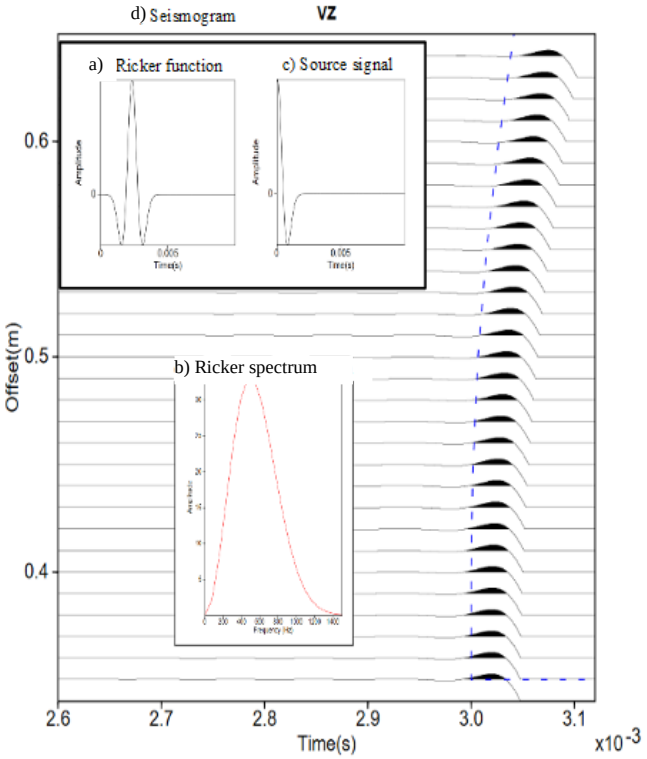

Figure 3 : Simulation results with finite differences in the case of homogeneous medium; a) Ricker function; b) Ricker function spectrum; c) Source signal used in finite difference simulations; d) The vertical velocity wavefield recovered at the receivers. The estimated arrival times computed by using the method presented in section 3 are plotted dashed curve

Now that we have verified that in the case of a homogeneous medium, the arrival times estimated with the model presented in section 3 fit well with the signals calculated with finite differences, we can examine the case of vertical stratification. In a second numerical test, we are interested in an extreme case where the depth is 1.5 m and where the difference in propagation velocity in the two media varies very strongly.

b)

We consider two homogeneous media characterized by constant velocity v_1 = 500 m/s and v_2 = 1000 m/s of dimensions x = 1.5 m and z = 1.5 m. The source is a Ricker function with the maximum at time t = 0s (Figure 5.a) like the previous simulation. A set of 15 receivers is located at the bottom of the model at z = 1.5 m. The first receiver is located at x = 0.75 m and z = 1.5 m, the distance between receivers is 0.05 m and the change of media is at x= 0.4 m and then at x= 1.1 m. We observe the propagation of the wavefront on the figure 4. The vertical velocity wave-field recovered at the receivers is presented in Figure 5.a. The estimated arrival times computed by using the method presented in section 3 are plotted on Figure 5.a (dashed curve).

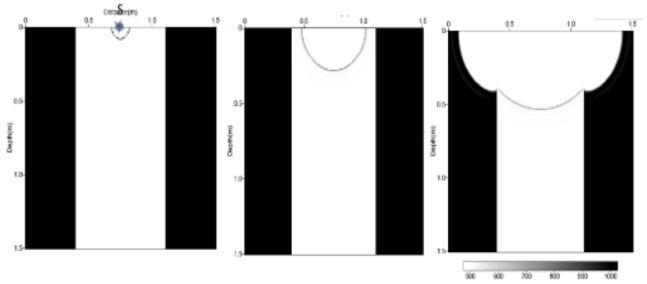

Figure 4 : Picture of the wavefront propagation in the finite difference simulation in the case of vertical stratification, the star indicates the source located at x=0.75, z=0. m .

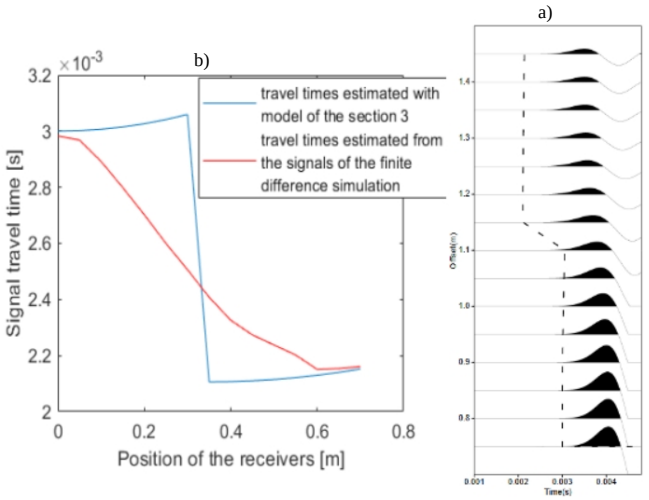

Figure 5 : Simulation results with finite differences in the case of vertical stratification; a) The vertical velocity wavefield recovered at the receivers. The estimated arrival times computed by using the method presented in section 3 are plotted dashed curve; b) Comparison of the travel times between the model estimate of section 3 and the estimate on the signals from the finite differences.

In order to compare the travel times accurately, we need to estimate the arrival times on the signals from the finite difference simulation. When we look at the signals in detail, we see a distortion, especially at x= 1.1 m at the boundary of the two media. Following this observation, the question is how to calculate precisely the arrival times of distorted signals from the finite difference simulation. The answer is not obvious. Here, we decide to pick the first arrival breaking point to get an idea of travel times (Figure 5.b).
We find that both models fit well for the sensors closest away from the source, and also for the sensors farthest away from the change of medium outside the trench. In contrast, in the proximity of the boundary of the two media we observe differences. For the model of section 3 there is a brutal variation whereas on the finite difference data there is a continuous variation.
The objective would be to understand these differences in order to improve the simplified modeling presented in section 3, maybe by considering multiple paths. This is the subject of our current work. The goal is to obtain a simplified formulation of the analytical travel time estimate but sufficiently accurate for our problem at the meter scale. The next step of our work is to test the model of section 3 on real data in a controlled test area.

5 Conclusion

Following our results obtained on real data considering a homogeneous propagation medium, presented in a previous work [3], we presented here, an evolution of our time modeling, and we compared it to a finite difference modeling of the full-wave field. In this study, we presented two numerical experiments. The first medium is a simple homogeneous model. The second is more complex medium with vertical stratification in order to take into account the trench. We presented the calculation of the Cramer-Rao bound which is an essential tool to understand the impact of each parameter on the accuracy of the depth estimate. We compared our temporal modeling to a complete modeling of the wave field estimated by finite differences. We have noted the limits of our estimate of the travel time. We will now have to understand these limits to improve our temporal modeling. In our comparison with the finite differences the question arises of the calculation of the arrival time of distorted signals. We will be able to evolve the time modelisation by looking at possible multiple paths. In addition, we plan to test our temporal modeling on real data from a controlled test area.

Acknowledgments

This project is supported by CIFRE contract between MADE-SA and CNRS-UMR7330, CEREGE, from the ANRT French program of CNRS (Agence National de la Recherche Technique). This project is partially supported by RICE (Research & Innovation Center of Energy), GRTgaz.

References

[1] Y. Liu, D. Habibi, D. Chai, X. Wang, H. Chen, Y. Gao, S. Li, 2020, A Comprehensive Review of Acoustic Methods for Locating Underground Pipelines, *Applied sciences*, Vol. 10, No. 3 , art. No. 1031, DOI. 10.3390/app10031031

[2] J.M. Muggleton, E. Rustighi, Mapping the Uderworld : recent developments in vibro-acoustic techniques to locate buired

infrastructure, 2013, *Geotechnique Letters*, Vol. 3, No. 3, pp. 137-141, DOI. 10.1680/geolett.13.00032

[3] W. Xerri, G. Saracco, G. Gassier, L. Zomero, P. Picon, 2021, Preliminary Acoustic Study of 3D Localization of Buried Polyethylene Pipe, *Annual Review of Progress in Quantitative Nondestructive Evaluation*, Vol. 1, art. 74945, DOI.10.1115/QNDE2021-74945

[4] S. Operto, J. Virieux, A. Ribodetti & J. E. Anderson, 2009, Finite-differ-ence frequency-domain modeling of viscoacoustic wave propagation in two-dimensional tilted transversely isotropic media, *Geophysics*, 74(5), T75–T95, DOI: 10.1190/1.315724

[5] Y. Liu, D. Habibi, D. Chai, X. Wang, H. Chen, 2019, A Numerical Study of Axisymmetric Wave Propagation in Buried Fluid-Filled Pipes for Optimizing the Vibro-Acoustic Technique When Locating Gas Pipelines, *Energies*, Vol. 12, No.19, art. No. 3707, DOI. 10.3390/en12193707

[6] P. Stoica and A. Nehorai, 1989, MUSIC, maximum likelihood, and Cramer-Rao bound", *IEEE Transactions on Acoustics, Speech, and Signal Processing*, Vol. 37, No. 5, pp. 720-741, DOI. 10.1109/29.17564

[7] J. Virieux, P-SV wave propagation in heterogeneous media: Velocity-stress finite-difference method, 1989, *Geophysics*, Vol. 51, No. 4 , pp. 889–901, DOI. 10.1190/1.1442147

[8] G. H. F. Gardner, L. W. Gardner, A. R. Gregory, 1974, Formation velocity and density – The diagnostic basics for stratigraphic traps, Geophysics, Vol. 39, No. 6, pp. 770-780, DOI. 10.1190/1.1440465

[9] E. Forgues, G. Lambaré, Parameterization study for acoustic and elastic ray+Born inversion, 1997, *Journal of Seismic Exploration*, Vol. 6 , pp. 253-278

[10] J. Virieux, S. Operto, 2009, An overview of full-waveform inversion in exploration geophysics, Geophysics, Vol. 74, No. 6, pp. 127-152, DOI. 10.1190/1.3238367

[11] H. Igel, Computational Seismology, A Practical Introduction, Oxford University Press (2017)

[12] J.-P. Berenger, 1984, A perfectly matched layer for the absorption of electromagnetic waves, Journal of Computational Physics, Vol. 114, No. .2, pp. 185-200, DOI. 10.1006/jcph.1994.1159